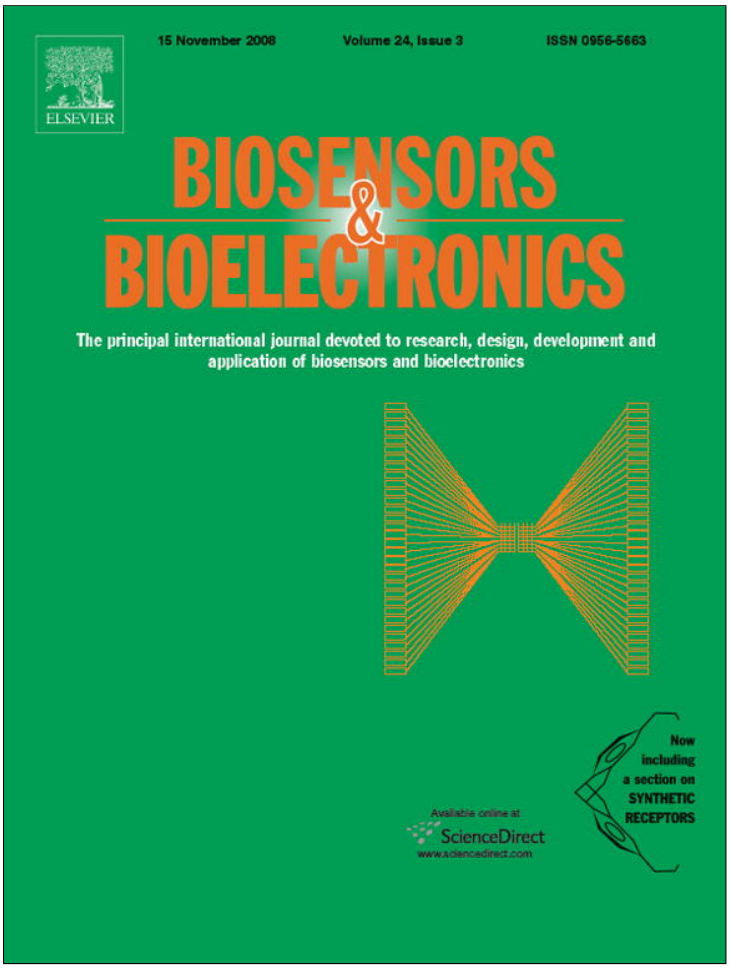

Biosensors and Bioelectronics 24 (2008) 461–466

Contents lists available at ScienceDirect

Biosensors and Bioelectronics

journal homepage: www.elsevier.com/locate/bios

Phage-based label-free biomolecule detection in an opto-fluidic ring resonator

Hongying Zhu, Ian M. White, Jonathan D. Suter, Xudong Fan*

Department of Biological Engineering, University of Missouri, 240D Bond Life Sciences Center, 1201 East Rollins Street, Columbia, MO 65211, United States

ARTICLE INFO

Article history:
Received 29 December 2007
Received in revised form 4 April 2008
Accepted 29 April 2008
Available online 9 May 2008

Keywords:
Optical biosensor
Whispering gallery mode
Virus detection
Label-free
Opto-fluidic ring resonator
Filamentous phage

ABSTRACT

We have developed a sensitive and inexpensive opto-fluidic ring resonator (OFRR) biosensor using phage as a receptor for analyte detection. Phages have distinct advantages over antibodies as biosensor receptors. First, affinity selection from large libraries of random peptides displayed on phage provides a generic method of discovering receptors for detecting a wide range of analytes with high specificity and sensitivity. Second, phage production can be less complicated and less expensive than antibody production. Third, phages withstand harsh environments, reducing the environmental limitations and enabling regeneration of the biosensor surface. In this work, filamentous phage R5C2, displaying peptides that bind streptavidin specifically, was employed as a model receptor to demonstrate the feasibility of a phage-based OFRR biosensor. The experimental detection limit was approximately 100 pM streptavidin and the $K_{d(apparent)}$ is 25 pM. Specificity was verified using the RAP 5 phage, which is not specific to streptavidin, as the negative control. Sensing surface regeneration results show that the phage maintained functionality after surface regeneration, which greatly improves the sensors' reusability. The phage-based OFRR biosensor will become a promising platform for universal biomolecule detection with high sensitivity, low cost, and good reusability.

1. Introduction

Label-free optical biosensors, such as highly sensitive surface plasmon resonance (SPR) instruments (Homola, 2008; Hoa et al., 2007) and interferometers (Yemti et al., 2007; Schipper et al., 1998) allow real-time detection of biomolecular interactions without fluorescent labeling, which is time consuming and may change the properties of the analytes. However, SPR and interferometer biosensors are large and complicated, needing external microfluidics to transport the samples to the sensing surface and/or a delicate optical detection system that must be precisely aligned to yield usable results. With the aim to make a sensitive integrated sensing platform that can be integrated into a lab-on-a-chip device or micro-total analysis system, we developed a novel label-free optical sensing platform based on an opto-fluidic ring resonator (OFRR) (White et al., 2006; Suter et al., 2007; Zhu et al., 2007a, 2008). It successfully integrates the ring resonator with microfluidics, allowing for real-time biomolecule detection. Fig. 1(A) and (B) diagram the principle of the OFRR. It utilizes a micro-sized quartz capillary as the microfluidics and each cross-section of the capillary forms a ring resonator. The ring resonator supports a series of optical resonant modes called whispering gallery modes or circulating waveguide modes (WGMs) that circulate along the resonator surface. The capillary wall is sufficiently thin (<4 μm) so that the evanescent field of the resonant WGMs extends into the core by about 100 nm and interacts with the analyte in the capillary core. The evanescent interaction between the resonant WGMs and the analyte near the inner surface enables detection without fluorescent or radioactive labeling. The resonant wavelength of the WGM λ is determined by (Gorodetsky and Ilchenko, 1999):

$$2\pi n_{\text{eff}} r = m\lambda, \tag{1}$$

where n_{eff} is the effective refractive index (RI) of the medium experienced by WGMs, r is the ring radius, and m is an integer multiple indexing the WGM. A change in RI at the sensor surface, due either to change in the RI of the bulk solution or to binding of analyte molecules to immobilized receptors, will change n_{eff}, causing a corresponding change in resonant wavelength λ. Because of the high Q factors (~10^7) in the OFRR, photons circulate thousands of times around the ring resonator circumference, greatly increasing interaction between the evanescent wave and surface-bound analyte and thus improving sensitivity. The OFRR principle has been demonstrated for protein, DNA and virus detection (Zhu et al., 2007a, 2008; Suter et al., 2007) with a protein detection limit of several picomolar, corresponding to a mass detection limit of a few pg/mm^2, comparable to commercialized SPR instruments.

In addition to sensitivity, specificity and robustness of receptors are another two important characteristics in biosensor

* Corresponding author. Tel.: +1 573 884 2543; fax: +1 573 884 9676.
E-mail address: fanxud@missouri.edu (X. Fan).

0956-5663/$ – see front matter © 2008 Elsevier B.V. All rights reserved.
doi:10.1016/j.bios.2008.04.028

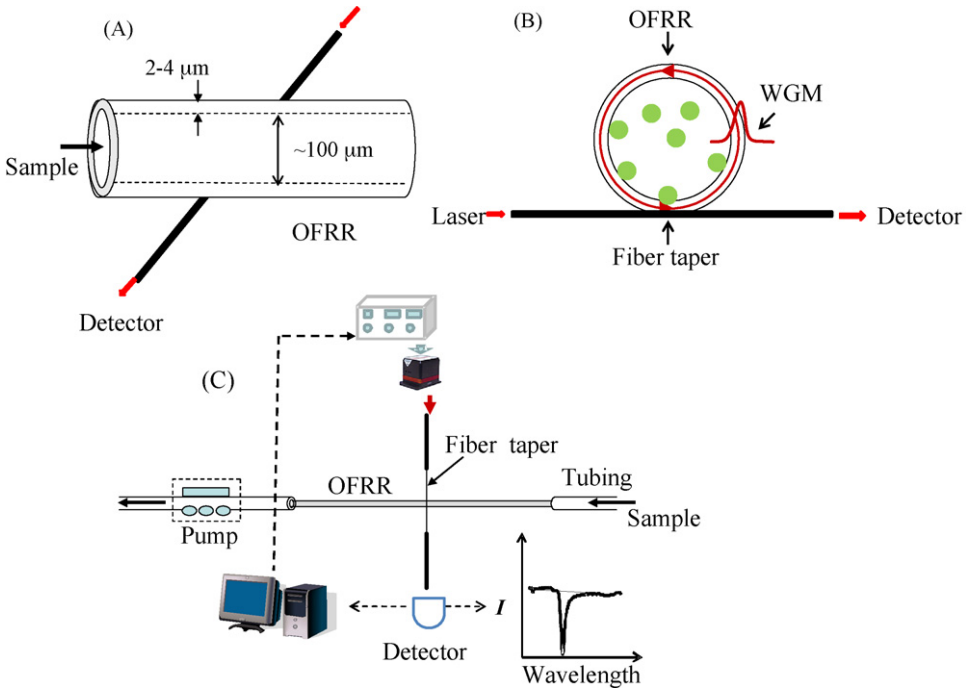

Fig. 1. (A) The OFRR employs a micro-sized glass capillary with thin wall (<4 μm) and (B) the capillary cross section forms the ring resonator. The WGM circulates along the OFRR circumference. Its evanescent field extends beyond the interior surface of the OFRR and interacts with the analytes in the core. (C) Overall experimental setup for biomolecule detection.

development. Antibodies are the most commonly used receptors in biosensor applications, but they are expensive to produce and tend to denature in unfavorable conditions, such as might be encountered in environmental field testing. Therefore, there is a need for a cheaper, more robust type of receptor. The development of phage display technology has drawn increasing attention to the advantages of phages as biosensor receptors. Peptide-bearing phage that bind a given target biomolecule with high affinity and specificity can be affinity selected from large phage libraries displaying billions of random peptides, and can serve as receptors for detection of that biomolecule. Phage receptors can be produced by cheap, generic fermentation processes, and can withstand high temperature (up to 70 °C), extreme pH (2–12), and denaturants (up to 6 M urea). Nevertheless, they have so far found only limited application in biosensor development (Yang et al., 2006; Nanduri et al., 2007a,b,c; Ionescu et al., 2007; Petrenko and Vodyanoy, 2003; Olsen et al., 2006; Jia et al., 2007; Souza et al., 2006). For label-free optical biosensors in particular, phage has only been applied in SPR with a detection limit of 1 pM for β-galactosidase detection (Nanduri et al., 2007a). Although, SPR instrument is very sensitive and readily commercialized for decade, it is very expensive and may be not affordable in some applications. In order to develop a sensitive and inexpensive label-free optical biosensor with high specificity and selectivity, we explored the feasibility of using phage as receptors on OFRR sensing surfaces for universal biomolecule detection, combining the merits of the OFRR and phages receptors.

Streptavidin was chosen as the model analyte for this work phage clone R5C2, displaying a streptavidin-binding peptide on ~100 of its major coat protein (pVIII) subunits, served as the specific (analyte-binding) receptor; while phage clone RAP 5, displaying a non-streptavidin-binding peptide, served as a negative control receptor. OFRR biosensors in which the phages were covalently attached to the sensing surface were able to detect the streptavidin analyte with high sensitivity and specificity, and could be regenerated and used repeatedly. These results support phage-based OFRR biosensors as a promising new platform for analyte detection and quantitation.

2. Experimental methods

2.1. Materials

Ethanol, hydrofluoric acid (HF, 48%), 12 M HCl, anhydrous methanol, 3-aminopropyltrimethoxysilane (3-APS), 75% glutaraldehyde and bovine serum albumin (BSA) were purchased from Sigma-Aldrich (St. Louis, MO). All chemical agents were used without purification. Streptavidin (molecular weight 55 kDa) (from *Streptococcus avidinii*) was purchased from Invitrogen. Filamentous phages R5C2 (Chen et al., 2004) and RAP 5 (Mattews et al., 2002) were purified as described (Smith and Scott, 1993). The specific receptor phage R5C2 displays the streptavidin-binding peptide NH_2–ANRLPCHPQFPCTSHE, while the negative control receptor phage RAP 5 displays the control (non-streptavidin-binding) peptide NH_2–APTEWCPPHRTCWPTT. Both clones were affinity-selected from library f88–Cys5 (GenBank Accession AF246454). These filamentous virions have a rod-like structure 1.3 μm in length and 6 nm in diameter. Chemicals for the surface regeneration buffer – KSCN (0.46 M), $MgCl_2$ (1.83 M), urea (0.92 M), guanidine–HCl (1.83 M) and EDTA (20 mM) – were purchased from Sigma–Aldrich (St. Louis, MO) and used without further purification.

2.2. Experimental setup

OFRR fabrication is described in detail in previous work (White et al., 2006; Zhu et al., 2007b). In brief, a quartz capillary was pulled under intense heat (~2000 °C) provided by CO_2 lasers, after which diluted HF (~10%) was pumped through the capillary to reduce the wall thickness to a few micrometers. The experimental setup for the biomolecule detection was similar to previous work (Zhu et al., 2007a), as shown in Fig. 1(C). The OFRR was in contact with

an optical fiber taper with a diameter of approximately 3 μm. The taper delivered light from a 980 nm tunable diode laser from New Focus (San Jose, CA; linewidth <3 fm). The output wavelength of the laser is periodically scanned at a rate of 5 Hz. A photodetector was placed at the output end of the optical fiber to collect the optical intensity. When the laser wavelength meets the resonant condition described in Eq. (1), the light is coupled into the OFRR, causing a reduction in power measured at the fiber output, which can be used to indicate the WGM spectral position. The measurement system was controlled by a computer through a data acquisition card from National Instruments (Austin, TX) and the WGM spectral position was recorded for post-analysis.

2.3. OFRR bulk refractive index sensitivity (BRIS) characterization

Our theory to derive the density of bound analyte from the amount of resonance wavelength λ shift (Eq. (2) below) requires knowledge of the OFRR surface's BRIS (Zhu et al., 2007a). It is therefore essential to determine BRIS prior to the biomolecule detection. For this purpose, ethanol/water mixtures with gradually increasing concentrations of ethanol were pumped through the OFRR, causing the WGM resonant dips to shift to progressively longer wavelengths as the bulk RI in the core increases. BRIS is determined prior to each individual experiment. A representative figure with BRIS of 20 nm per refractive index units (RIU) for the OFRR used in one experiment was deduced by measuring the slope of the WGM shift versus RI change (see Fig. 1 in Supplementary Materials).

2.4. Immobilization phage on the sensing surface

Phages were covalently coupled to the sensor surface according to the scheme shown in Fig. 2 in Supplementary Materials. The interior surface of the OFRR was cleaned with HCl/methanol (v:v=50:50) mixture for 10 min and thoroughly rinsed with DI water. Then 1% 3-APS in water was passed through the OFRR for 20 min to aminate the surface. The OFRR was then thoroughly rinsed with water. The amine-reactive homobiofunctional crosslinker glutaraldehyde (5% in water) was pumped through the capillary for 20 min to functionalize the aminated surface. The OFRR was rinsed with water and PBS buffer was introduced into the OFRR to establish the detection baseline for subsequent experiments. Then phages in PBS buffer were pumped through the OFRR using syringe pump at the flow rate of 20 μL/min for 30 min to allow them to couple to the functionalized surface through their amine groups, after which the surface was rinsed with PBS buffer to remove non-coupled phages. Then the unoccupied sites were blocked with bovine serum albumin (BSA, 1 mg/mL) solution, followed by a PBS rinse. Finally, the OFRR was filled with PBS buffer and ready for detection of streptavidin.

3. Results and discussion

3.1. Theoretical basis for biomolecule detection

We have established a linear relationship between the magnitude of the WGM spectral shift and the molecule density on the OFRR surface (Zhu et al., 2007a), as shown in Eq. (2):

$$\delta\lambda = \sigma_p \alpha_{ex} \frac{2\pi\sqrt{n_2^2 - n_3^2}}{\varepsilon_0 \lambda} \frac{n_2}{n_3^2} S, \quad (2)$$

where $\delta\lambda$ is the amount of WGM spectral shift due to the biomolecules binding to the sensing surface, σ_p is the molecular surface density per unit area, α_{ex} is the excess polarizability of the analyte, n_2 =1.45 is the RI of the OFRR wall, and n_3 = 1.33 is the RI of the aqueous medium. ε_0 is vacuum permittivity, λ is the wavelength of the WGM, and S is the BRIS of the OFRR (in units of nm/RIU). The excess polarizability for phage and streptavidin is $4\pi\varepsilon_0 \times (5.1 \times 10^{-18})\,\mathrm{cm}^3$ and $4\pi\varepsilon_0 \times (3.2 \times 10^{-21})\,\mathrm{cm}^3$, respectively (Arnold et al., 2003; Zhu et al., 2008). When the surface is fully covered with phage, the phage surface density is 1.3×10^{10} virions/cm^2; when the surface is fully covered with streptavidin, the streptavidin surface density is 5×10^{12} molecules/cm^2 (streptavidin dimensions are 4.5 nm × 4.5 nm × 5 nm). Using Eq. (2) and the above parameters, we can determine the biomolecule surface density from the amount of WGM spectral shift measured in experiments.

3.2. Optimization of phage immobilization

In most phage-display based biosensor configurations, such as SPR (Nanduri et al., 2007a,c) and quartz crystal microbalance (QCM) (Nanduri et al., 2007b), phage are immobilized on the sensing surface simply through direct passive physical adsorption. This is a very simple method, but it takes long time (1–3 h) to reach a stabilized signal. Furthermore, immobilized phages tend to detach from the silica sensing surface, especially during the regeneration step. To reduce the surface preparation time and strengthen attachment, phages were coupled to the silica surface covalently as outlined previously (Appendix B Fig. 2 in Supplementary Materials). Fig. 2(A) shows the real-time WGM spectral response for the phage bound to the surface at three different concentrations (10^{10}, 10^{11} and 10^{12} virion/mL. It took only approximately 15 min for the signal to reach the steady state, much less than for the physical adsorption method. This may be due to the high surface to volume ratio in the circular OFRR's microfluidics channel, which promotes faster phage diffusion to the sensing surface from the bulk solution. To find out the optimal phage concentration used for preparing the sensing surface, phage at different concentrations were tested on the sensing surface. The phage surface coverage was calculated from Eq. (2) using the amount of WGM spectral shift caused by phage immobilization. Fig. 2(B) shows that surface coverage increased gradually with increasing phage concentration, reaching a maximum of approximately 20% at 10^{12} virion/mL. The maximal coverage was relatively low compared to previous studies (Nanduri et al., 2007a). However, less phage surface coverage may give phage a more flexible conformation and spaces for binding, compared to the rigid and tight packing layers (Nanduri et al., 2007a).

3.3. Real-time detection of streptavidin

Fig. 3 shows the real-time response of a glutaraldehyde-functionalized OFRR sensor, first to R5C2 specific receptor phage at a concentration of 10^{11} virion/mL, then to the BSA blocker at a concentration of 1 mg/mL, and finally to the streptavidin analyte at a concentration of 1.8 μM. As expected, the resonance wavelength λ shifts to higher values as more virions or BSA molecules bound to the surface, or more analyte molecules captured by R5C2 receptors. The first of these shifts plateaus at a 38 pm, corresponding to 7.7% coverage of the sensor surface with receptor virions. The third shift plateaus at 9 pm, corresponding to 7.4% coverage of the surface with analyte molecules–very close to receptor virion coverage. This result suggests that each receptor virion is almost fully covered with analyte molecules at saturation.

3.4. Binding specificity

To ensure that the response from Fig. 3 was due to the specific binding between the phage and streptavidin, the sensing

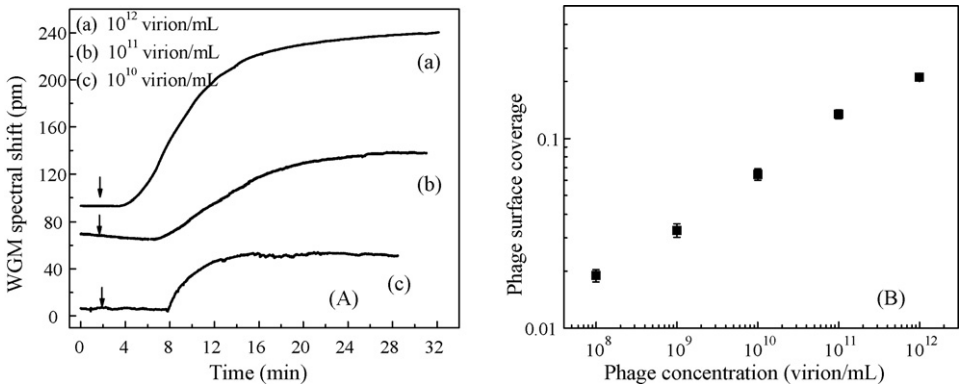

Fig. 2. Optimization of phage immobilization. (A) Real-time sensorgram for phage immobilization at different concentration. Arrows indicate the time when phage was introduced into the OFRR. Curves are vertically shifted for clarity. (B) Estimated phage surface coverage vs. phage concentration. Each experiment was repeated four times.

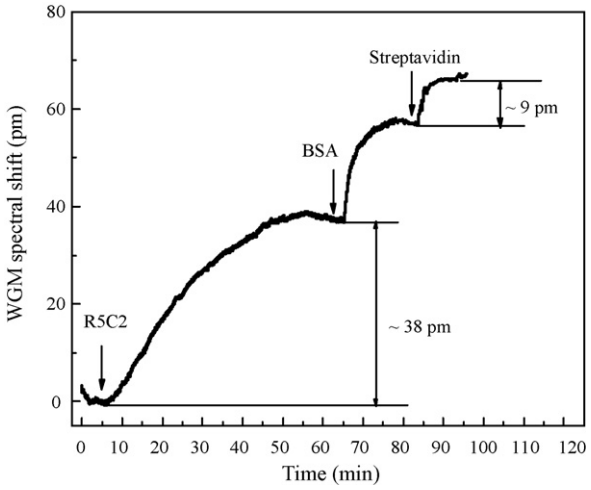

Fig. 3. Sensorgram for streptavidin detection. The interior surface of OFRR was immobilized with working phage probes R5C2, and then the unoccupied sites were blocked with BSA. Finally, the sensing surface was exposed to 1.8 μM streptavidin.

signal was compared for the streptavidin-specific phage R5C2 and the negative control phage RAP 5. Phages were coupled to the surface at a concentration of 10^{11} virion/mL. Fig. 4(A) shows no observable response to streptavidin when the negative control phage was used as the probe, but a strong response when the streptavidin-specific phage was used as probe. A competitive binding assay further verified the specificity of the sensing results. Phages were coupled to the sensing surface at a concentration of 10^{12} virion/mL. Streptavidin at a concentration of 1.8 μM was preincubated for 20 min with free R5C2 phage at concentrations ranging from 10^4 to 10^{11} virion/mL before being pumped through the R5C2 coated OFRR. We expected higher concentrations of free phage in the preincubation solution to result in less free streptavidin in solution. Fig. 4(B) shows that, as expected, the normalized streptavidin surface coverage (streptavidin surface coverage divided by phage surface coverage) decreased progressively with increasing free phage concentrations. These two assays confirm that the interaction between streptavidin and the R5C2 phage is highly specific.

3.5. Detection limit and dynamic range

To explore the detection limit and dynamic range, streptavidin at concentrations ranging from 0.18 nM to 3.6 μM were passed consecutively through the OFRR. The surface was rinsed with PBS buffer after each sample injection to minimize the sensing signal caused by bulk refractive index change and non-specific binding. The normalized streptavidin surface coverage gradually increased and finally reached the saturation level. From Fig. 5, the normalized streptavidin surface coverage was linear on the log-log scale within the concentration range of 0.9 nM to 3.6 μM. The lowest concentration used in experiment was 0.18 nM, causing 0.65 pm

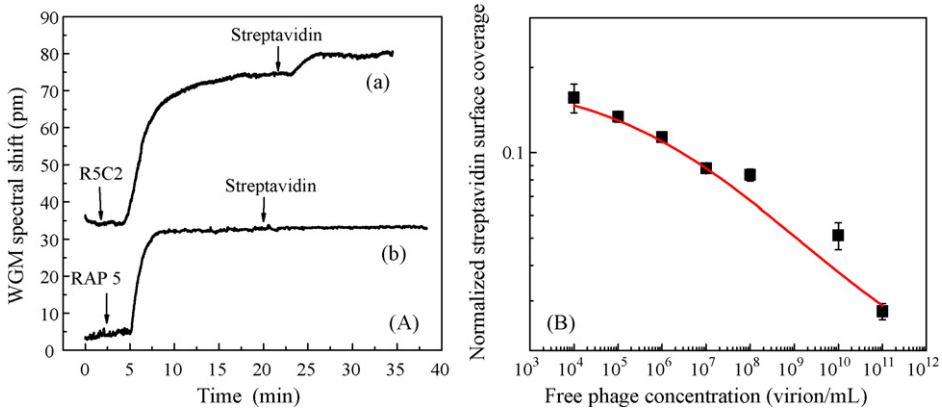

Fig. 4. (A) Sensing specificity test. (a) The OFRR response with working phage R5C2 and (b) the OFRR response with negative control phage RAP 5. (B) Competitive binding assay for phage specificity test. WGM spectral responses to the phage probe on the sensing surface to the streptavidin (1.8 μM). Strepavidin was incubated with free phage (10^{11}–10^4 virion/mL) prior to exposure to sensing surface. Each experiment was repeated three times.

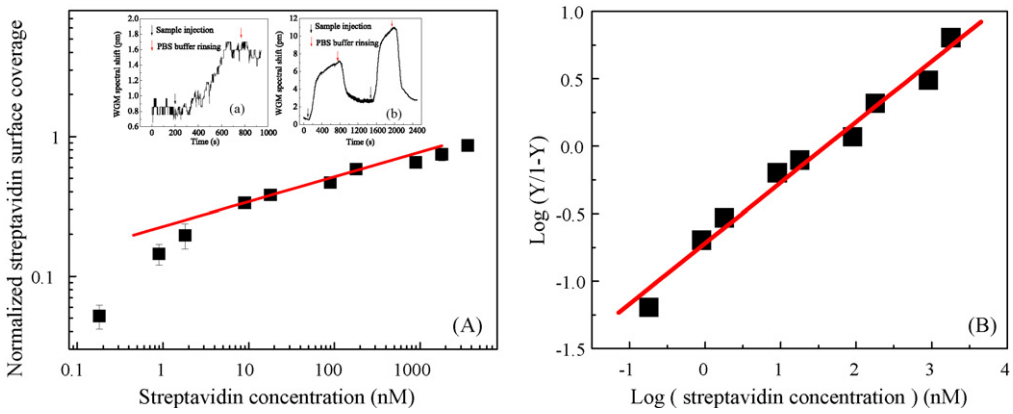

Fig. 5. (A) The normalized streptavidin surface coverage vs. streptavidin concentration when working phage R5C2 was used as receptor on the OFRR surface. Each experiment was repeated four times. The inset (a) is the real-time WGM spectral shift for 0.18 nM streptavidin and (b) is the real-time WGM spectral shift for 1.8 μM and 3.6 μM streptavidin. Solid line is the linear fit ($R = 0.94$). (B) Hill plot of binding isotherm showing the ratio of occupied and free phages as a function of streptavidin concentration. Solid line is the linear fit. ($n = 0.4494 \pm 0.02472$, $K_{d(apparent)} = 25$ pM, $R = 0.99$).

WGM spectral shift. The theoretical detection limit is limited by the spectral resolution, which in turn is limited by the Q-factor and temperature fluctuation. A spectral resolution of 0.02 pm for the OFRR has been achieved earlier (Fan et al., 2007), which leads to a theoretical detection limit of about 5 pM, similar to the detection limit achieved by SPR ~1 pM (Nanduri et al., 2007a) and QCM ~3 pM (Nanduri et al., 2007b). The detection limit of OFRR can probably be improved by at least another order of magnitude by several available means. First, the sensitivity of the OFRR can be further increased by improving OFRR manufacture procedures. In current experimental setup, the HF acid etching procedure results in the roughness on capillary interior surface, thus decreasing the resonance Q-factor and limiting the spectral resolution. The capillary can be made by using a fiber drawer tower without further HF etching, which helps maintain the Q-factors of the OFRR. Second, sandwich assay detection method can be employed. In this method, the biotinylated phage is immobilized on the sensing surface as the primary receptor to trap streptavidin, and then secondary biotinylated phage can be introduced to the sensing surface to amplify the sensing signal. Additionally surface chemistry for phage immobilization can also be further improved. Currently the surface functionalization method relies on an unstable Schiff base that can compromise the probe immobilization. We can use stabilizing agent such as sodium cyanoborohydride to reduce the Schiff base into stable secondary or tertiary amine bond, which might increase phage surface coverage.

3.6. Binding affinity

Binding between phage receptors and their target analytes has been quantified by Petrenko and Vodyanoy (2003). Applied to the present work, the interaction can be expressed as

$$[\mathrm{Ph}] + n[\mathrm{Str}] \Leftrightarrow [\mathrm{PhStr}_n], \tag{3}$$

in which the [Ph] is the density of free phage on the OFRR surface, [Str] is the concentration of free streptavidin in solution, and $[\mathrm{PhStr}_n]$ is the density of the phage-streptavidin complex on the OFRR surface, n is the number of streptavidin bound to a phage. The Hill equation for this interaction is described as follows:

$$\log\left(\frac{Y}{1-Y}\right) = \log K_a + n \log[\mathrm{Str}], \tag{4}$$

where $Y/1-Y$ is the ratio of the occupied phages to the free phages on the sensing surface, K_a is the association constant. The Hill plot shows $\log(Y/1-Y)$ versus log[Str], in which $Y = R/R_{max}$, where R is the average normalized streptavidin surface coverage. From this, we can estimate the apparent value of the associate constant K_a of the interaction of streptavidin with phage from the intercept of the Hill plot (Nanduri et al., 2007b). Fig. 5(B) shows the Hill plot for the binding process in Fig. 5. According to the Hill plot, the apparent value of dissociation constant $K_{d(apparent)}$, which is defined as $1/K_a$ (Samoylov et al., 2002), is estimated to be approximately 25 pM and the Hill coefficient, n, is 0.45. The apparent value of dissociation constant is in agreement with what is typically obtained for phage probes and their corresponding targets (9 pM to 26 nM (Nanduri et al., 2007a,c; Petrenko and Vodyanoy, 2003; Samoylov et al., 2002).

3.7. Surface regeneration

As discussed before, the bacteriophage is very robust and can withstand harsh environments, such as high temperature and extreme pH. This leads to a long sensor lifetime and a high number of uses without the need to perform the surface functionalization and phage immobilization before each reuse. To reuse the sensor, it is required that all residual analyte molecules be stripped from the sensor surface after each assay without removing receptors or compromising their ability to bind analyte. There are a few standard procedures for regenerating antibody receptors, but none so far for regenerating phage receptors. Here we explored two multi-ingredient stripping cocktails based on work with SPR sensors (Andersson et al., 1999). One was ionic solution made up by KSCN (0.46 M), $MgCl_2$ (1.83 M), urea (0.92 M), and guanidine-HCl (1.83 M); the other was a chelating solution made by 20 mM EDTA solution. Mg^{2+} interacts with EDTA to form Mg^{2+}–EDTA complex. The Mg^{2+}–EDTA works with other chaotropic agents, such as guanidine–HCl, urea, and the SCN^- ions, so that the dissociation between the target and probe will be increased (Andersson et al., 1999). The cocktail stock solutions were mixed with water by volume ratio of 1:1:1. As shown in Fig. 6, the mixed solution was pumped through the sensor capillary after streptavidin binding. Its high RI caused a large resonance wavelength shift, but the signal returned almost to baseline when the sensor was subsequently rinsed with PBS buffer, indicating complete removal of streptavidin analyte from the surface. When the same concentration of streptavidin was applied to the stripped surface, the

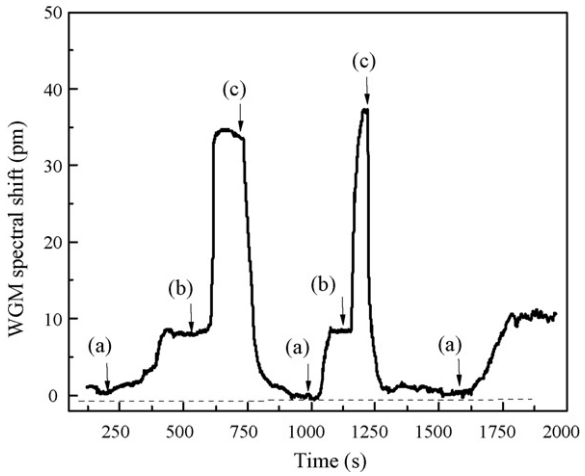

Fig. 6. Sensorgram in response to sensing surface regeneration. (a) Injection of 1.8 μM streptavidin that binds to the sensing surface, (b) injection of cocktail regeneration solution to remove streptavidin from the sensing surface and (c) injection of PBS buffer to rinse off the cocktail regeneration solution and re-establish the detection baseline. Dashed line is the sensing baseline.

resonance wavelength shift was nearly the same as that observed before stripping, indicating complete regeneration of the sensor. The regeneration was repeated yet again, with similar results. The sensor can be used for many times if only the analyte is stripped off the receptor. If the sensor surface needs to be completely regenerated which means the receptor need to be removed and immobilize new receptors. Diluted HF (<1%) acid will be used to etch the interior surface. In this case the sensor could be used for 4 to 5 times until the capillary wall is etched through by HF acid.

4. Conclusion

In this work, we developed a sensitive and robust label-free OFRR sensor in which filamentous phages bearing analyte-binding peptides served as the immobilized receptors. The experimental detection limit for the model analyte, streptavidin, was found to be approximately 100 pM, and the sensitivity could probably be improved at least another order of magnitude by available means. The sensing surface could be regenerated for reuse by passing a stripping cocktail through the sensor. Such sensors have an extraordinarily wide range of applications, since phages displaying peptides that bind a great variety of analytes – including threat agents and clinically relevant biomarkers – can be affinity selected from available large random-peptide libraries. In future work, the application of phage as receptor in biosensor application will be further explored, including increasing the sensor sensitivity and extending its application in clinical research.

Acknowledgements

The authors thank George Smith for purified phage, and both him and Shaohui Zhang for helpful discussion. Financial support was provided by the 3M Non-Tenured Faculty Award and the Wallace H. Coulter Foundation Early Career Award.

Appendix A. Supplementary data

Supplementary data associated with this article can be found, in the online version, at doi:10.1016/j.bios.2008.04.028.

References

Andersson, K., Hämäläinen, M., Malmquist, M., 1999. Analytical Chemistry 71, 2475–2481.
Arnold, S., Khoshsima, M., Teraoka, I., Holler, S., Vollmer, F., 2003. Optics Letters 28, 272–274.
Chen, L., Zurita, A.J., Ardelt, P.U., Giordano, R.J., Arap, W., Pasqualini, R., 2004. Chemistry and Biology 11, 1081–1091.
Fan, X., White, I.M., Zhu, H., Suter, J.D., Oveys, H., 2007. Proceeding of SPIE. 6452, 64520M.
Gorodetsky, M.L., Ilchenko, V.S., 1999. Journal of the Optical Society of America B 16, 147–154.
Homola, J., 2008. Chemical Review 108, 462–493.
Hoa, X.D., Kirk, A.G., Tabrizian, M., 2007. Biosensors and Bioelectronics 27, 151–160.
Ionescu, R.E., Cosnier, S., Herrmann, S., Marks, R.S., 2007. Analytical Chemistry 79, 8662–8668.
Jia, Y., Qin, M., Zhang, H., Niu, W., Li, X., Wang, L., Li, Xin., Bai, Y., Cao, Y., Feng, X., 2007. Biosensors and Bioelectronics 22, 3261–3266.
Mattews, L.J., Davis, R., Smith, G.P., 2002. The Journal of Immunology 169, 837–846.
Nanduri, V., Balasubramanian, S., Sista, S., Vodyanoy, V.J., Simonian, A.L., 2007a. Analytical Chimica Acta 589, 166–172.
Nanduri, V., Sorokulova, I.B., Samoylov, A.M., Simonian, A.L., Petrenko, V.A., Vodyanoy, V., 2007b. Biosensors and Bioelectronics 22, 986–992.
Nanduri, V., Bhunia, A.K., Tu, S.I., Paoli, G.C., Brewster, J.D., 2007c. Biosensors and Bioelectronics 23, 248–252.
Olsen, E.V., Sorokulova, I.B., Petrenko, V.A., Chen, I.H., Barbaree, J.M., Vodyanoy, V., 2006. Biosensors and Bioelectronics 21, 1434–1442.
Petrenko, V.A., Vodyanoy, V.J., 2003. Journal of Microbiological Methods 53, 253–262.
Samoylov, A.M., Samoylova, T.I., Hartell, M.G., Pathirana, S.T., Smith, B.F., Vodyanoy, V., 2002. Biomolecular Engineering 18, 269–272.
Schipper, E.F., Rauchalles, S., Kooyman, R.P.H., Hock, B., Greve, J., 1998. Analytical Chemistry 70, 1192–1197.
Smith, G.P., Scott, J.K., 1993. Methods in Enzymology 217, 228–257.
Suter, J.D., White, I.M., Zhu, H., Shi, H., Caldwell, C.W., Fan, X., 2007. Biosensors and Bioelectronics 23, 1003–1009.
Souza, G.R., Christianson, D.R., Staquicini, F.I., Ozawa, M.G., Snyder, E.Y., Sidman, R.L., Miller, J.H., Arap, W., Pasqualini, R., 2006. Proceedings of the National American Society 103, 1215–1220.
White, I.M., Oveys, H., Fan, X., 2006. Optics Letters 31, 1319–1321.
Yemti, A., Greve, J., Lambeck, P.V., Wink, T., van Hövell, S.W.F.M., Beumer, T.A.M., Wijin, R.R., Heideman, R.G., Subramaniam, V., Kanger, J.S., 2007. Nano Letters 7, 394–397.
Yang, L.C., Tam, P.Y., Murray, B.J., Mclntire, T.M., Overstreet, C.M., Weiss, G.A., Penner, R.M., 2006. Analytical Chemistry 78, 3265–3270.
Zhu, H., White, I.M., Suter, J.D., Dale, P.S., Fan, X., 2007a. Optics Express 15, 9139–9146.
Zhu, H., White, I.M., Suter, J.D., Zourob, M., Fan, X., 2007b. Analytical Chemistry 79, 930–937.
Zhu, H., White, I.M., Suter, J.D., Zourob, M., Fan, X., 2008. The Analyst 132, 356–360.